Current **A**pplied **S**cience and **T**echnology e-ISSN: 2586-9396

Curr. Appl. Sci. Technol. 2025, Vol. 25 (No.25), e0263873

Research article

Analysis of Optical Dynamics and Spectroscopic Phenomena of Praseodymium-doped Phospho-Tellurite Glasses for Visible Luminescence Devices

Wiraphat Thanyaphirak[1,2], Patarawagee Yasaka[1,2] *, Kitipun Boonin[1,2], Kanlayaphad Jarupreedephad[2] and Jakrapong Kaewkhao[1,2]

[1]Center of Excellence in Glass Technology and Materials Science (CEGM), Nakhon Pathom Rajabhat University, Nakhon Pathom 73000, Thailand
[2]Physics Program, Faculty of Science and Technology, Nakhon Pathom Rajabhat University, 73000, Thailand

Received: 1 July 2024, Revised: 24 September 2024, Accepted: 21 November 2024, Published: 28 March 2025

Abstract

The glasses prepared with praseodymium oxide (Pr_2O_3) in phosphor-tellurite glass systems with varying compositions were used to study their emission behavior. The compositions investigated range from the base glass (40-x)TeO_2 - 30P_2O_5 - 20ZnO - 10Sb_2O_3 to the glass with the addition of praseodymium oxide at different concentrations, represented by the parameter x. The main objective of this research was to understand the influence of praseodymium oxide on the optical and spectroscopic properties of the glass matrices. The glass samples were prepared using conventional melt-quenching techniques at 1100°C for 30 min, annealing at 300°C for 3 h, and characterization using various analytical methods. Changes in physical properties of the glass due to the addition of praseodymium were recorded and analyzed. It was observed that the addition of praseodymium decreased densities from 4.15 to 3.90 g/cm^3, and refractive index from 1.653 to 1.633. However, the molar volume increased from 36.5 to 39.2 cm^3/mol. The existence of the glass host (phospho-tellurite) and its physical characteristics were confirmed by FTIR and XRD analysis. Optical absorption spectra were recorded to investigate the peaks associated with transitions from $^3H_4$ state to $^3P_{2,1,0}$, $^1D_2$, $^1G_4$, and $^3F_{4,3,2}$ states. Photoluminescence (PL) spectra were measured to study the emission characteristics, including the emission peaks ($^3P_0 \rightarrow {}^3H_4$, $^3P_1 \rightarrow {}^3H_5$, $^1D_2 \rightarrow {}^3H_4$, $^3P_0 \rightarrow {}^3F_2$, and $^3P_1 \rightarrow {}^3F_3$). At concentrations above 0.1 mol % of Pr^{3+} ions, the emission intensities are found to decrease with the increase of Pr^{3+} concentration due to concentration quenching. Additionally, the CIE chromaticity coordinates, ranging from orange to green, were determined to assess the suitability of glasses for visible luminescence devices.

Keywords: phospho-tellurite; praseodymium; luminescence; melt-quenching; glass

*Corresponding author: E-mail: pyasaka@hotmail.com
https://doi.org/10.55003/cast.2025.263873

1. Introduction

Glass, an amorphous solid material (Mahdy et al., 2023), has been an integral part of technological advancements due to its unique physical and chemical properties. Its versatility allows for a wide range of applications, from everyday use in household items to sophisticated roles in advanced optical and electronic devices. The ability to tailor glass properties through the incorporation of various dopants has significantly expanded its functionality and performance. Doping glass with rare earth elements, such as praseodymium oxide (Pr_2O_3), introduces remarkable enhancements in its optical and spectroscopic properties, making it a material of interest for numerous scientific and industrial applications (Rajaramakrishna et al., 2018; Kolavekar & Ayachit, 2022).

One of the most compelling aspects of glass is its application in optical and photonic devices. The transparency of glass at a broad range of wavelengths, combined with its ease of fabrication into complex shapes and structures, makes it an ideal candidate for lenses, optical fibers, and waveguides. Moreover, the introduction of dopants can fine-tune the glass's refractive index, absorption, and emission characteristics, which are crucial for applications in lasers, amplifiers, and sensors. For instance, rare earth-doped glasses have been extensively used in the development of laser materials because rare earths have the unique ability to emit light upon stimulation, offering high efficiency and diverse emission wavelengths.

In the realm of glass luminescence materials, the incorporation of praseodymium oxide into glass matrices holds significant promise. Praseodymium ions have a complex energy level structure and exhibit multiple electronic transitions (Rao et al., 2020) that can be controlled for efficient light emission. Specifically, the Pr^{3+} ions show transitions from the ground state $^3H_4$ to various excited states such as $^3P_0$, $^3P_1$, $^3P_2$, and $^1D_2$ (Carnall et al., 1968), which are responsible for the visible emission spectra. This characteristic makes praseodymium-doped glasses suitable for applications in lighting diodes or laser technologies, where control over emission spectra is desired.

In this study, the emission behavior of praseodymium oxide (Pr_2O_3) in phospho-tellurite glass systems with varying compositions was focused. By preparing glass samples through conventional melt-quenching techniques and analyzing their physical, structural, optical, and luminescence properties, the aim was to understand how different concentrations of praseodymium oxide influenced these characteristics. The investigation included detailed analysis using FTIR and XRD to confirm the glass structure, as well as optical absorption and photoluminescence spectroscopy to study the emission behavior. Additionally, the CIE chromaticity coordinates were determined to evaluate the potential of these glasses for visible luminescence applications. Through this research, we sought to contribute to the development of advanced luminescent materials and expand the applications of praseodymium-doped glasses in various technological fields.

2. Materials and Methods

Glass samples for this investigation were fabricated through the melt-quenching technique, encompassing a range of compositions denoted by the formula $(40\text{-}x)TeO_2\text{-}30P_2O_5\text{-}10Sb_2O_3\text{-}20ZnO\text{-}xPr_2O_3$, where x ranged from 0.0 to 1.5 mol%, giving the glass formula the name PTeSZPrx. The starting materials, TeO_2, P_2O_5, Sb_2O_3, ZnO, and Pr_2O_3, were accurately weighed and blended in six distinct 10-gram batches. Each batch was thoroughly stirred in a crucible to ensure homogeneity and then heated to 1100°C at a heating rate of 4.58°C/min using an electric furnace. Once the molten mixture reached the

desired temperature, it was immediately poured into preheated graphite molds and annealed at 300°C for 3 h to relieve internal stresses. After annealing, the samples were cut into precise dimensions of 1.0 × 1.5 × 0.3 cm³ for the comprehensive investigation of their properties. The preparation process is shown in Figure 1.

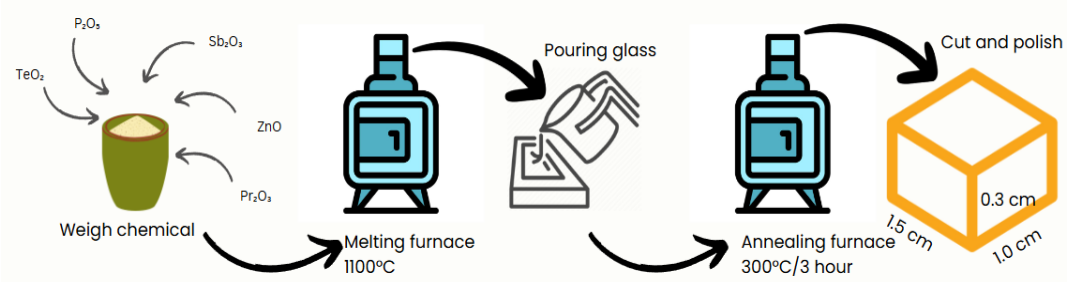

Figure 1. Preparation process

The density (ρ) of the samples was determined using a densitometer (model AND HR-200) by accurately weighing the specimens. The refractive index (n) was measured using a Presidium Refractive Index Meter II. The structural properties of the samples were assessed through X-ray diffraction (XRD) analysis, employing a Rigaku SmartLab X-ray Diffractometer. To investigate the vibrational states of the phospho-tellurite glasses, Fourier transform infrared spectra (FTIR) analysis was conducted using a Nicolet™ iS™5 FTIR spectrophotometer. UV-Vis-NIR absorption spectra were recorded using a UV-3600 Shimadzu UV-VIS-NIR spectrophotometer. Additionally, the photoluminescent properties of the samples were examined. Excitation, emission, and lifetime spectra were measured using an Agilent Cary Eclipse fluorescence spectrometer. This comprehensive analysis provided detailed insights into the optical and spectroscopic behavior of the praseodymium oxide-doped phospho-tellurite glasses, facilitating the understanding of their potential applications in luminescence devices. The entire characterization of PTeSZPrx glasses is effectively summarized in Figure 2.

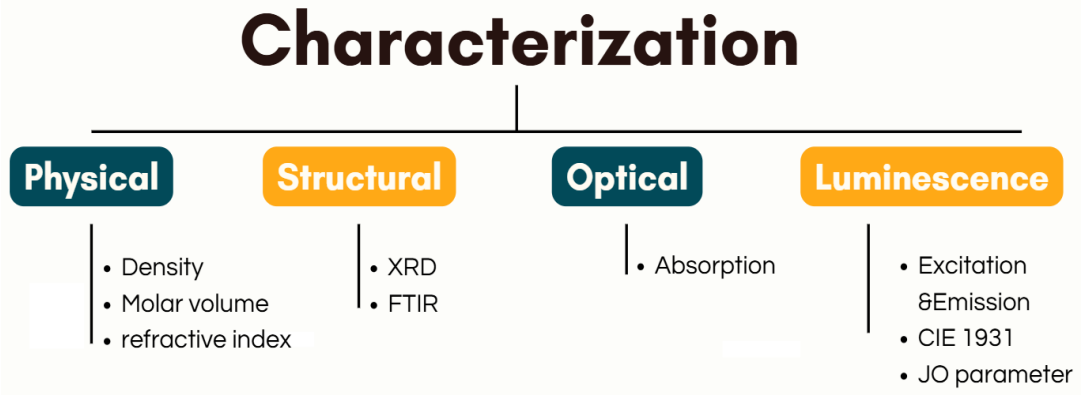

Figure 2. Characterization of PTeSZPrx glasses

3. Results and Discussion

3.1 Physical properties

Density is a critical and fascinating parameter in glass science, and is sensitive to minute variations in the glass matrix composition. It reflects the structural changes occurring within the glass and is crucial for determining both physical and optical properties. The comparison of experimental and empirical density values also highlights the amorphous or non-crystalline nature of the glasses. In the current study, changes in density with varying Pr_2O_3 concentrations, as shown in Figure 3, indicate a decrease as Pr_2O_3 content was increased. The decrease in density was likely due to structural changes, such as an increase in non-bridging oxygens (NBOs) that disrupt the glass network (Sadeq & Morshidy, 2019). Similarly, the refractive index of the PTeSZPr glass samples was reduced by raising the concentration of Pr_2O_3. The increase in NBOs resulted in a decrease in the refractive index due to a decrease in the density of bond packing within the glass matrix, which allowed light to pass through more easily. In contrast, the trend in molar volume showed an increase with higher Pr_2O_3 concentrations. This suggests that the introduction of Pr_2O_3 led to a more open glass structure, emphasizing the significant impact of Pr_2O_3 on the glass network. The rise in molar volume was ascribable to the larger ionic radius of praseodymium in contrast to tellurium. The substitution of TeO_2 by Pr_2O_3 created excess free volume due to the size difference between the praseodymium and tellurium atoms (Colak, 2023).

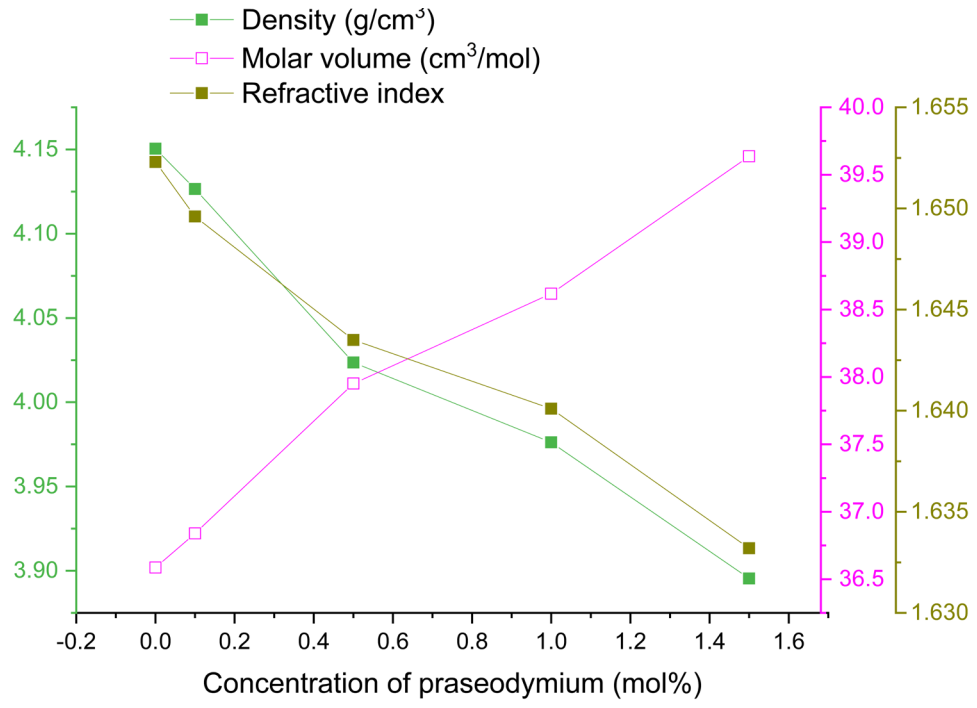

Figure 3. Density, molar volume, and refract index of PTeSZPr glasses

3.1 Physical properties

The X-ray diffraction (XRD) analysis verified the amorphous nature of the examined glasses. The scattering angles ranged from 10° to 80°, as shown in Figure 4, which included the XRD patterns for powdered PTeSZPr0.0, PTeSZPr0.1, PTeSZPr0.5, PTeSZPr1.0, and PTeSZPr1.5 samples. Across all glass samples, no distinct diffraction peaks were observed. Instead, a diffuse background between 20° and 35° was evident, highlighting the amorphous characteristics of the samples. This diffuse pattern supported the uniformity and consistency of the process of glass-forming, demonstrating the successful creation of an amorphous glass structure across all compositions studied (Mahdy et al., 2023).

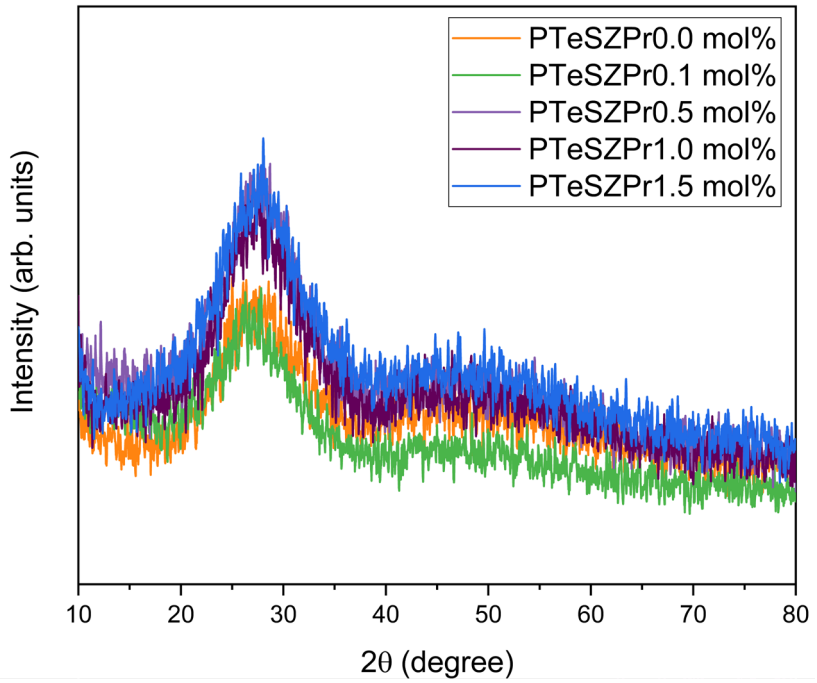

Figure 4. XRD pattern of PTeSZPr glasses

FTIR spectroscopy is a technique used to study the interaction between infrared radiation and materials, providing insights into their functional groups and chemical bonds. Figure 5 shows the FTIR spectrum for the PTeSZPr glasses, with the observed peaks summarized in Table 1. As shown in Table 1, nearly all samples exhibit five prominent peaks. The peak at 501 cm^{-1} is due to Te–O–Te or O–Te–O bond bending vibrations (Azaludin & Sabri, 2021). The peak identified at 625 cm^{-1} is associated with the vibrational modes of Te–O bonds in TeO_4 units, specifically involving bridging oxygen atoms with Te–O (Azaludin & Sabri, 2021). The peak at 905 cm^{-1} corresponds to P–O–P bonds asymmetric stretching vibrations in linear metaphosphate chains (Farag et al., 2022). Additionally, the bands around 1626 cm^{-1} and between 2500-3500 cm^{-1} are linked to various O–H bond vibrations (Selvi et al., 2017), indicative of the hygroscopic nature of phosphate glass, which results in O–H bond vibrations.

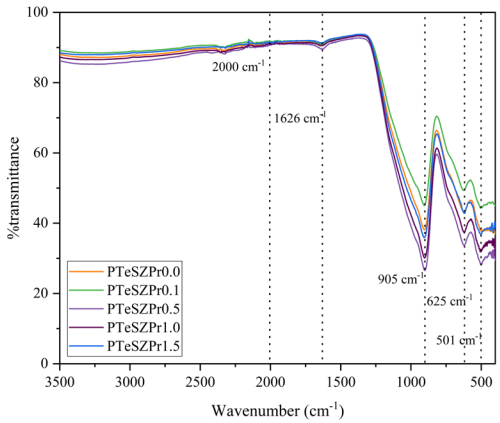

Figure 5. FTIR spectra of PTeSZPr glasses

Table 1. Assignments of FTIR band

Band position (cm^{-1})	Assignments	Reference
501	Te–O–Te or O–Te–O bond bending vibrations	(Azaludin & Sabri, 2021)
625	Vibrations of TeO_4 linkage occur between TeO_4 units and the bridging oxygen.	(Azaludin & Sabri., 2021)
905	P–O–P bonds asymmetric stretching vibrations linked with linear metaphosphate chain	(Farag et al., 2022)
1626, 2500-3500	Vibrations of O–H bonds	(Selvi et al., 2017)

3.3 Optical properties

Figure 6 displays the optical absorption spectra of PTeSZPr glasses spanning 350-2500 nm. The absorption characteristics of rare earth (RE) ions in a glass matrix depend on their local environment and interactions with surrounding ligands. As depicted in Figure 6, eight absorption bands are observed at 444, 468, 482, 589, 1009, 1434, 1526, and 1937 nm. These bands correspond to transitions from the Pr^{3+} ion's $^3H_4$ ground state to the $^3P_2$, $^3P_1$, $^3P_0$, $^1D_2$, $^1G_4$, $^3F_4$, $^3F_3$, and $^3F_2$ excited states ($4f^2 \rightarrow 4f^2$ intra-configurational transitions) (Carnall et al., 1968) The consistent positions of these absorption bands across all PTeSZPr samples indicate a uniform ligand field and a homogeneous distribution of Pr^{3+} ions. Notably, the $^3H_4 \rightarrow (^3F_4, ^3F_3, ^3F_2)$ and $^3H_4 \rightarrow ^3P_2$ transitions are particularly intense and classified as "hypersensitive." These transitions adhere to the selection rules $\Delta S = 0$, $|\Delta L| \leq 2$, and $|\Delta J| \leq 2$, and their intensity is significantly influenced by the local environment of the Pr^{3+} ions, impacting the magnitude of the JO parameters (Ω_2, Ω_4, and Ω_6). The strong absorption bands below 500 nm enhance pumping efficiency under blue light excitation, which is advantageous for visible light emissions. The broad absorption bands in PTeSZPr glasses are primarily due to the significant variation in crystal field strengths across different sites.

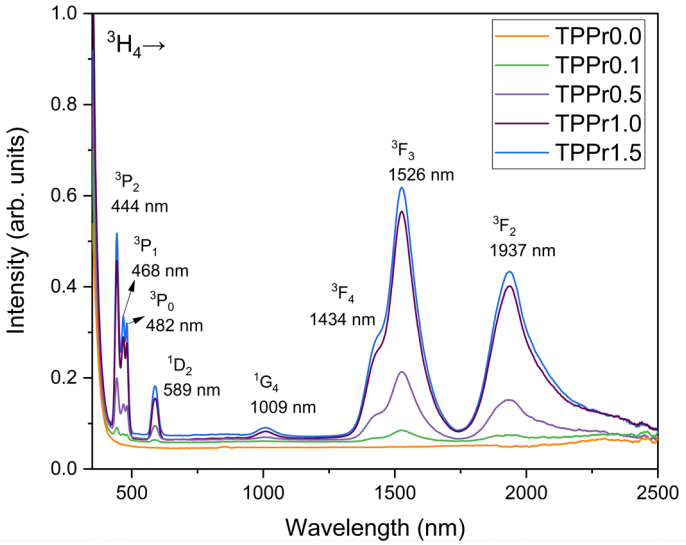

Figure 6. Absorption spectra of PTeSZPr glasses

3.4 Luminescence properties

The luminescence properties of Pr^{3+} doped PTeSZPr glasses were explored by recording the excitation spectra with the emission wavelength (λ_{em}) fixed at 602 nm, as illustrated in Figure 7. The spectra reveal three excitation bands at 444, 469, and 482 nm, which correspond to the $^3H_4\rightarrow{}^3P_0$, $^3P_1$, and $^3P_2$ transitions, respectively. The most intense band at 444 nm was selected for excitation in the emission spectra recordings for all PTeSZPr glasses, illustrated in Figure 8. The emission spectra, captured in the visible region, display several broad and inhomogeneous bands peaking at 489, 527, 602, 644, and 688 nm, corresponding to the transitions $^3P_0\rightarrow{}^3H_4$, $^3P_1\rightarrow{}^3H_5$, $^1D_2\rightarrow{}^3H_4$, $^3P_0\rightarrow{}^3F_2$, and $^3P_1\rightarrow{}^3F_4$, in that order. The band at 602 nm shows the highest luminescence intensity, which rises with Pr^{3+} ion content up to 0.1 mol%, then reduces because of luminescence quenching. On the other hand, the emission at 489 nm continues to rise with Pr^{3+} ion content up to 1.0 mol%, after which it is also quenched. This quenching is caused by non-radiative processes such as multi-phonon relaxation and cross-relaxation channels (Rao et al., 2020). Changes in the emission intensity of various bands as the concentration of RE^{3+} ions varies are influenced by the distribution of energy levels featuring small energy gaps (Rao et al., 2020). This distribution facilitates non-radiative transitions aided by phonon energy within these levels, as depicted in Figure 9. This leads to different quenching points for various bands.

The luminescence emission colors of PTeSZPr glasses, when excited at 444 nm, were analyzed using the CIE chromaticity coordinates derived from the emission spectra. As shown in Figure 10, these coordinates remained relatively stable across different concentrations of Pr^{3+} ions. The color coordinate of PTeSZPr glass is initially located in the orange range. However, as the Pr^{3+} ion content rises, the color coordinate shifts to white and eventually to green, due to quenching effects at various concentrations for each emission peak.

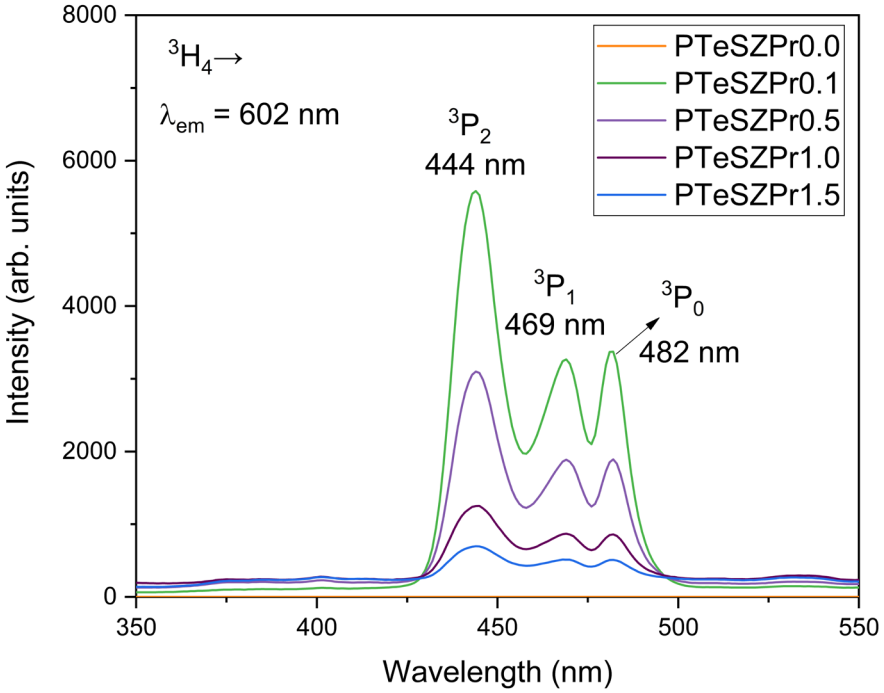

Figure 7. Excitation spectra of PTeSZPr glasses

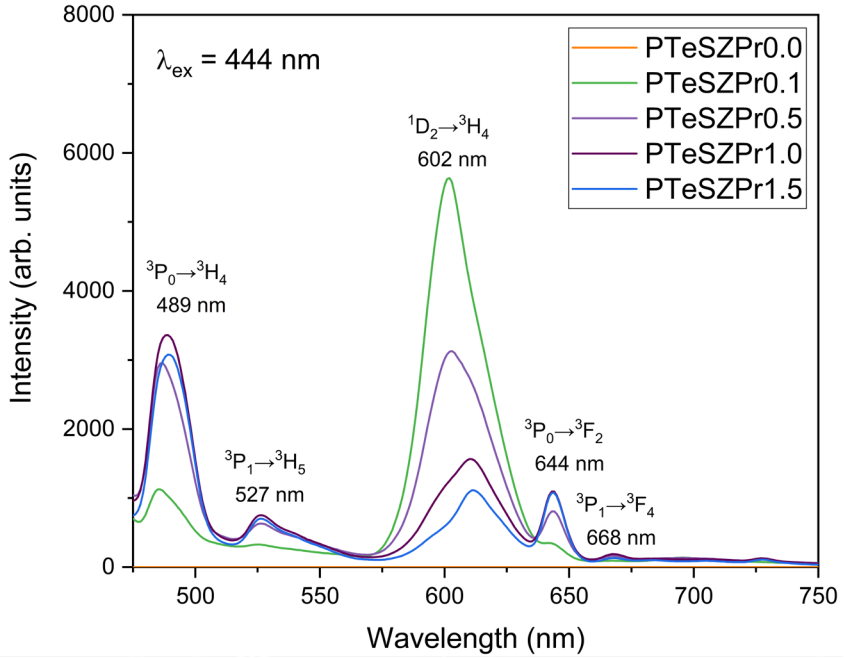

Figure 8. Emission spectra of PTeSZPr glasses

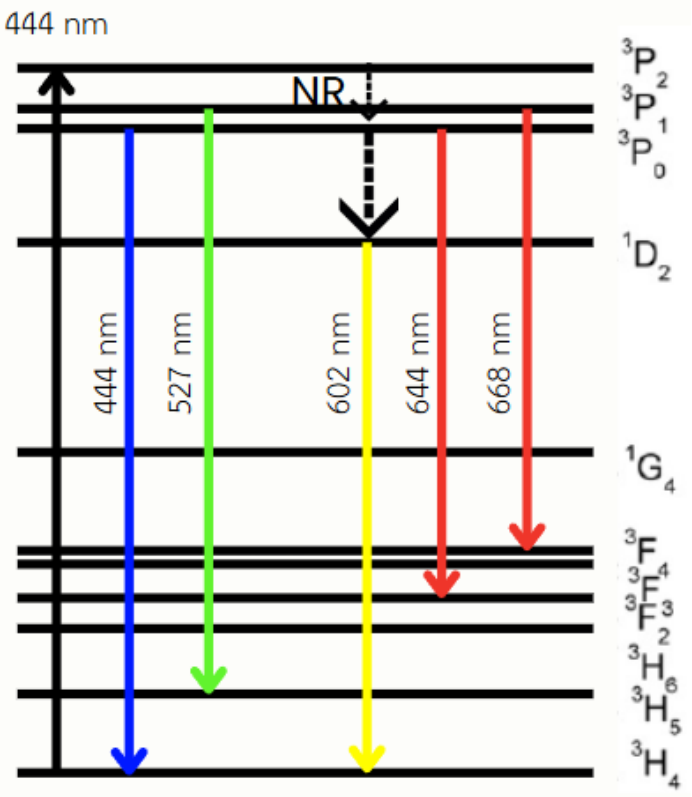

Figure 9. Energy level diagram for Pr^{3+} ions in PTeSZPr glasses

To understand the optical properties of Pr^{3+} doped PTeSZPr glasses, an analysis of the Judd-Ofelt (JO) parameters was essential. A comparison of the experimental oscillator strengths (f_{exp}) with the calculated ones (f_{cal}) from existing literature (Aryapriya et al., 2020) revealed a strong correlation, as shown by the low root mean square (δ_{rms}) deviations in Table 2, confirming the JO theory's validity. The JO parameters Ω_2, Ω_4, and Ω_6 were determined through a least-squares fitting procedure (Aryapriya et al., 2020) and the results are displayed in Table 3. The parameter Ω_2 is indicative of structural disorder around the dopant rare-earth (RE) ion, related to the asymmetry of the ligand field, and it remains stable with increasing Pr^{3+} ion concentration. In contrast, Ω_4 and Ω_6 are linked to the glass matrix's intrinsic properties, such as viscosity and rigidity, and are influenced by ligand-atom vibrations. The highest values for these parameters were observed in the PTeSZPr1.5 glass, while the lowest was in the PTeSZPr0.1 glass. Ω_2 also suggests a covalent bond between RE and oxygen, with larger values indicating more polarized and asymmetric sites within the glasses. As shown in Table 3, Ω_2 increases with higher Pr_2O_3 concentrations, implying greater asymmetry at higher doping levels compared to other hosts. This increase in Ω_2 indicates a covalent bond formation between Pr^{3+} and oxygen atoms, proportional to the ligands' polarizability due to coulombic interactions involving the induced dipoles and quadruple of the RE ions in the PTeSZPr glasses.

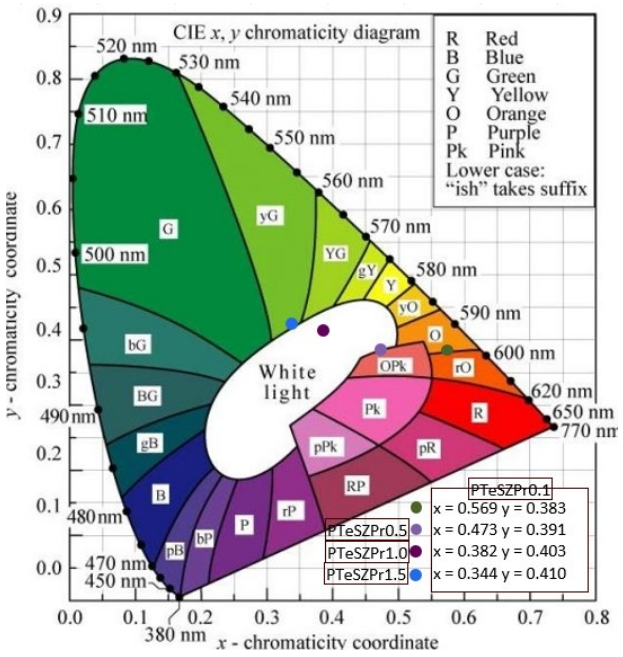

Figure 10. CIE 1931 diagram of PTeSZPr glasses

Table 2. Oscillator strength (f_{exp} & f_{cal}), least square fitting (δ_{rms}) value

Transition $^3H_4 \rightarrow$	PTeSZPr0.1		PTeSZPr0.5		PTeSZPr1.0		PTeSZPr1.5	
	f_{exp} ($\times10^{-6}$)	f_{cal} ($\times10^{-6}$)	f_{exp} ($\times10^{-6}$)	f_{cal} ($\times10^{-6}$)	f_{exp} ($\times10^{-6}$)	f_{cal} ($\times10^{-6}$)	f_{exp} ($\times10^{-6}$)	f_{cal} ($\times10^{-6}$)
$^3P_2$	1.1853	0.7103	6.6173	5.7560	21.4851	22.7527	19.5642	20.2717
$^3P_1$	0.4521	0.4055	5.0640	4.4518	11.5751	11.1737	7.4314	7.4478
$^3P_0$	0.4176	0.3987	3.9826	4.3777	10.4488	10.9875	7.2864	7.3237
$^1D_2$	0.3506	0.2160	3.4831	1.7888	7.0949	7.0537	6.8705	6.2874
$^3F_3$	1.1506	1.1824	10.0204	10.1200	38.9358	38.8683	34.2960	34.2762
$^3F_2$	0.3619	0.3589	4.7708	4.7636	19.8283	19.8373	18.6125	18.6133
δ_{rms}	0.203		0.832		0.585		0.376	

Table 3. Comparison of $\Omega_{2,4,6}$ with reports on other glasses in the literature

Code name	Ω_2	Ω_4	Ω_6	Trend	Ref.
PTeSZPr0.1	0.01	0.61	1.12	$\Omega_6 > \Omega_4 > \Omega_2$	Present work
PTeSZPr0.5	2.69	6.78	8.66	$\Omega_6 > \Omega_4 > \Omega_2$	Present work
PTeSZPr1.0	19.98	17.06	36.94	$\Omega_6 > \Omega_2 > \Omega_4$	Present work
PTeSZPr1.5	22.71	11.43	34.12	$\Omega_6 > \Omega_2 > \Omega_4$	Present work
BPr3	2.35	1.74	25.89	$\Omega_6 > \Omega_2 > \Omega_4$	(Teja et al., 2024)
2PrZTFB	7.69	1.82	9.75	$\Omega_6 > \Omega_2 > \Omega_4$	(Suthanthirakumar et al., 2017)
$PPbKANPr_{0.5}$	1.51	18.03	19.81	$\Omega_6 > \Omega_4 > \Omega_2$	(Basavapoornima et al., 2020)
NABPPr4	17.52	4.64	8.16	$\Omega_2 > \Omega_6 > \Omega_4$	(Sangwaranatee et al., 2020)
Pr^{3+}:$Sr_3Y_2(BO_3)_4$	10.57	2.94	17.85	$\Omega_6 > \Omega_2 > \Omega_4$	(Wei et al., 2009)

The lasing parameters including radiative transition probability (A), effective line width ($\Delta\lambda_{eff}$), stimulated emission cross-section (σ), and branching ratio (β_R) for the PTeSZPr glasses were determined using JO parameters, emission spectra, and refractive index values, employing theoretical models documented in the literature (Mitra & Jana, 2015; Aryapriya et al., 2020). Table 4 shows the calculated radiative parameters for the key emission transitions $^3P_0 \rightarrow {}^3H_4$ and $^1D_2 \rightarrow {}^3H_4$ of the studied glasses, alongside other reported PTeSZPr glasses. The energy extraction rate from laser materials is indicated by the stimulated emission cross-section (σ) of the emission bands, calculated with JO parameters. For the $^3P_0 \rightarrow {}^3H_4$ transition, the values are 0.604, 5.688, 13.564, and 8.877 ($\times 10^{-20}$ cm^2) for the PTeSZPr0.1, PTeSZPr0.5, PTeSZPr1.0, and PTeSZPr1.5 glasses, respectively. Among the studied glasses, the $^3P_0 \rightarrow {}^3H_4$ transition displays higher values of branching ratio (β_R) and stimulated emission cross-section (σ). Remarkably, PTeSZPr0.1 glass exhibits the highest β_R and σ values, highlighting its strong potential for laser applications comparable to other Pr^{3+} doped glasses.

4. Conclusions

The study of the phospho-tellurite glasses doped with praseodymium oxide (Pr_2O_3) demonstrated significant insights into their structural, physical, and luminescence properties. Structural integrity and amorphous nature, X-ray diffraction (XRD) and Fourier transform infrared spectroscopy (FTIR) analyses confirmed the amorphous nature of the glass samples. The XRD patterns showed no distinct diffraction peaks, and the FTIR spectra revealed characteristic peaks associated with the glass matrix components. For density and refractive index, the density of the PTeSZPr glasses decreased with a rising concentration of Pr_2O_3, attributed to the formation of non-bridging oxygens (NBOs). Similarly, the refractive index decreased due to reduced bond packing density, facilitating easier light passage. In the case of optical properties, the study of oscillator strengths and JO intensity parameters indicated good agreement between experimental and calculated values, validating the JO theory. The parameters Ω_2, Ω_4, and Ω_6 were indicative of the structural disorder and the nature of the bonds in the glasses. For luminescence behavior, the praseodymium-doped glasses exhibited significant luminescence emission when excited at 444 nm. The CIE chromaticity coordinates indicated a transition from orange to white and eventually to green as the Pr^{3+} ion increased. This shift was due to quenching effects at various emission peaks. As for potential for laser applications, among the prominent emission transitions, the $^3P_0 \rightarrow {}^3H_4$ transition had a higher branching ratio (βR) and stimulated emission cross-section (σ) values, especially for PTeSZPr0.1 glass. This suggests that PTeSZPr0.1 glass had a high potential for laser applications due to its superior luminescence properties

Table 4. The $^3P_0 \rightarrow {}^3H_4$ and $^1D_2 \rightarrow {}^3H_4$ transitions for of the PTeSZPr glasses and other reported glasses, emission band position (λ_P, nm), effective bandwidth ($\Delta\lambda_{eff}$, nm), transition probability (A, s^{-1}), calculated and experimental branching ratios (β_R), and stimulated emission cross-section ($\times 10^{-20}$ cm^2).

Transition	Parameter	PTeSZ Pr0.1	PTeSZ Pr0.5	PTeSZ Pr1.0	PTeSZ Pr1.5	0.75Pr ZTFB (Suthanthirakumar et al., 2017)	Pr-LP (Mitra & Jana, 2015)	PrPbLiFB (Balakrishna et al., 2017)
$^3P_0 \rightarrow {}^3H_4$	λ_p	489	489	489	489	486	485	488
	$\Delta\lambda_{eff}$	12.86	14.99	15.79	16.08	8.43	14.58	6.76
	A	2788	30386	75951	50200	16215	30380	19466
	σ	0.604	5.688	13.564	8.877	6.706	5.530	3.340
	β_R (exp)	0.046	0.256	0.461	0.566	0.511	0.328	0.250
	β_R (cal)	0.615	0.559	0.394	0.302	0.328	0.699	0.320
$^1D_2 \rightarrow {}^3H_4$	λ_p	602	602	602	602	613	600	604
	$\Delta\lambda_{eff}$	27.12	28.95	27.23	21.33	12.91	14.51	7.34
	A	1086	8276	35066	31942	1555	1129	3593
	σ	0.256	1.843	8.338	9.779	0.858	0.484	0.870
	β_R (exp)	0.9445	0.6942	0.436	0.305	0.264	0.966	0.700
	β_R (cal)	0.239	0.1524	0.182	0.192	0.286	0.975	0.480

5. Acknowledgements

The authors express gratitude to the Center of Excellence in Glass Technology and Materials Science (CEGM) for their invaluable support, including expertise and access to necessary equipment for this research.

6. Conflicts of Interest

The authors declare that they have no known competing financial interests or personal relationships that could have appeared to influence the work reported in this paper.

ORCID

Patarawagee Yasaka https://orcid.org/0000-0003-2392-046X

References

Aryapriya, N., Gopi, S., Krishnapriya, T., Jose, A., Saritha, A. C., Unnikrishnan, N. V., Joseph, C., & Biju, P. R. (2020). Concentration-dependent fluorescence and Judd–Ofelt analysis of trivalent-praseodymium-doped alkali fluoroborate glass. *Journal of Electronic Materials*, 49(6), 3624-3633. https://doi.org/10.1007/s11664-020-08053-6

Azaludin, N. R. M., & Sabri, N. S. (2021). Infrared spectroscopy of mixed glass former effect in borotellurite glasses: a review. *GADING Journal of Science and Technology*, 4(1), 94-102.

Balakrishna, A., Babu, S., Kumar, V., Ntwaeaborwa, O. M., & Ratnakaram, Y. C. (2017). Optical properties and spectroscopic study of different modifier based Pr^{3+}:LiFB glasses as optical amplifiers. *Spectrochimica Acta - Part A: Molecular and Biomolecular Spectroscopy*, 170, 167-173. https://doi.org/10.1016/j.saa.2016.07.013

Basavapoornima, C., Kesavulu, C. R., Maheswari, T., Pecharapa, W., Depuru, S. R., & Jayasankar, C. K. (2020). Spectral characteristics of Pr^{3+}-doped lead based phosphate glasses for optical display device applications. *Journal of Luminescence*, 228, Article 117585. https://doi.org/10.1016/j.jlumin.2020.117585

Carnall, W. T., Fields, P. R., & Rajnak, K. (1968). Electronic energy levels of the trivalent lanthanide aquo ions. I. Pr^{3+}, Nd^{3+}, Pm^{3+}, Sm^{3+}, Dy^{3+}, Ho^{3+}, Er^{3+}, and Tm^{3+}. *The Journal of Chemical Physics*, 49(10), 4424-4442. https://doi.org/10.1063/1.1669893

Colak, S. C. (2023). Soda-lime-silica glass structure with MoO_3 doping: An optical approach. *Optik*, 293, Article 171408. https://doi.org/10.1016/j.ijleo.2023.171408

Farag, M. A., Ibrahim, A., Hassaan, M. Y., & Ramadan, R. M. (2022). Enhancement of structural and optical properties of transparent sodium zinc phosphate glass–ceramics nano composite. *Journal of the Australian Ceramic Society*, 58(2), 653-661. https://doi.org/10.1007/s41779-022-00716-3

Kolavekar, S. B., & Ayachit, N. H. (2022). Impact of variation of TeO_2 on the thermal properties of lead borate glasses doped with Pr_2O_3. *European Physical Journal Plus*, 137(4), Article 475. https://doi.org/10.1140/epjp/s13360-022-02674-y

Mahdy, E. A., Alsaif, N. A. M., Rammah, Y. S., & Abo-Mosallam, H. A. (2023). Synthesis, thermal, structural, microhardness properties and gamma-ray attenuation efficiency of Cd^{2+} and Fe^{3+} Co-doped Na_2O-CaO-SiO_2 glasses. *Journal of Electronic Materials*, 52(8), 5492-5503. https://doi.org/10.1007/s11664-023-10474-y

Mitra, S., & Jana, S. (2015). Intense orange emission in Pr3+ doped lead phosphate glass. *Journal of Physics and Chemistry of Solids*, 85, 245-253. https://doi.org/10.1016/j.jpcs.2015.05.007

Rajaramakrishna, R., Wongdeeying, C., Yasaka, P., Limkitjaroenporn, P., Sangwaranatee, N., & Kaewkhao, J. (2018). Pr3+ doped BaO:ZnO:B_2O_3:TeO_2 glasses for laser host matrix. *Journal of Metals, Materials and Minerals*, 28(2), 47-54.

Rao, V. H., Prasad, P. S., & Babu, K. S. (2020). Visible luminescence characteristics of Pr3+ ions in TeO2–Sb2O3–WO3 glasses. *Optical Materials*, 101, Article 109740. https://doi.org/10.1016/j.optmat.2020.109740

Sadeq, M. S., & Morshidy, H. Y. (2019). Effect of mixed rare-earth ions on the structural and optical properties of some borate glasses. *Ceramics International*, 45(15), 18327-18332. https://doi.org/10.1016/j.ceramint.2019.06.046

Sangwaranatee, N. W., Kiwsakunkran, N., & Kaewkhao, J. (2020). Investigation on Physical and Optical of Praseodymium Doped Sodium Aluminium Barium Phosphate Glasses. *Journal of Physics: Conference Series*, 1428(1), Article 012031. https://doi.org/10.1088/1742-6596/1428/1/012031

Selvi, S., Marimuthu, K., & Muralidharan, G. (2017). Effect of PbO on the B_2O_3–TeO_2–P_2O_5–BaO–CdO–Sm_2O_3 glasses - Structural and optical investigations. *Journal of Non-Crystalline Solids*, 461, 35-46. https://doi.org/10.1016/j.jnoncrysol.2017.01.028

Suthanthirakumar, P., Basavapoornima, C., & Marimuthu, K. (2017). Effect of Pr3+ ions concentration on the spectroscopic properties of Zinc telluro-fluoroborate glasses for laser and optical amplifier applications. *Journal of Luminescence*, 187, 392-402. https://doi.org/10.1016/j.jlumin.2017.03.052

Teja, V. R., Sreenivasulu, M., & Chavan, V. K. (2024). Praseodymium ion-doped boro lithium glass material for optical applications: W-LED. *Journal of Materials Science: Materials in Electronics*, 35(2), Article 166. https://doi.org/10.1007/s10854-023-11897-3

Wei, Q., Li, X. Z., Wang, Z. J., & Long, X. F. (2009). Growth and spectroscopic properties of Pr3+ doped Sr 3y2(BO3)4 crystal. *Materials Research Innovations*, 13(1), 2-6. https://doi.org/10.1179/143307509X402093